LA-UR- 09-01940

Approved for public release;
distribution is unlimited.

Title:	The Mechanical Design and Dynamic Testing of the IBEX-Hi Electrostatic Analyzer Spacecraft Instrument
Author(s):	John D. Bernardin Allen G. Baca
Intended for:	2009 AIAA Infotech@ Aerospace & AIAA Unmanned Unlimited Conference

Los Alamos
NATIONAL LABORATORY
EST. 1943

Form 836 (7/06)

Mechanical Design and Dynamic Testing of the IBEX-Hi Electrostatic Analyzer Spacecraft Instrument

John D. Bernardin[1]
Los Alamos National Laboratory, Los Alamos, NM 87545

Allen G. Baca[2]
Sandia National Laboratory, Albuquerque, NM 87185-0521

This paper presents the mechanical design, fabrication and dynamic testing of an electrostatic analyzer spacecraft instrument. The functional and environmental requirements combined with limited spacecraft accommodations, resulted in complex component geometries, unique material selections, and difficult fabrication processes. The challenging aspects of the mechanical design and several of the more difficult production processes are discussed. In addition, the successes, failures, and lessons learned from acoustic and random vibration testing of a full-scale prototype instrument are presented.

I. Introduction

NASA's Interstellar Boundary Explorer (IBEX) is a mission designed to explore the physics of the interaction between the solar system's heliosphere and the gallaxy's interstellar medium through which the solar system is passing. At the heart of the IBEX mission is a sun-pointed, spinning satellite on a highly elliptical earth orbit. Two energetic neutral atom (ENA) imaging instruments, named IBEX-Hi and IBEX-Lo, are positioned on opposite sides of the satellite and are used to measure the population and energy density distributions of neutral particles emanating from the interaction zone.

The IBEX-Hi Instrument utilizes electro-optics to capture and analyze the high-energy spectrum of the ENAs. A brief summary of the design features and operation theory of the instrument can be described by referring to Fig. 1. At the donut-shaped entrance aperture of IBEX-Hi, particles attempt to enter and pass through a collimator. The collimator, consisting of a series of negatively and positively charged large aperture grids, repels ambient electrons and ions and allows ENAs from a narrow field of view to enter the instrument. After transiting through the collimator, the ENAs pass through an ultrathin (50-100Å thick) carbon charge-conversion foil where the ENA is stripped of an electron, yielding a net positively charged ion. The frames on which the carbon foils are mounted, are positively charged so-as to accelerate the charged ions downstream into an electrosatatic filter. This filter is formed from two concentric half-torroidal-shaped electrostatic analyzer (ESA) plates. An electrical field generated between the two

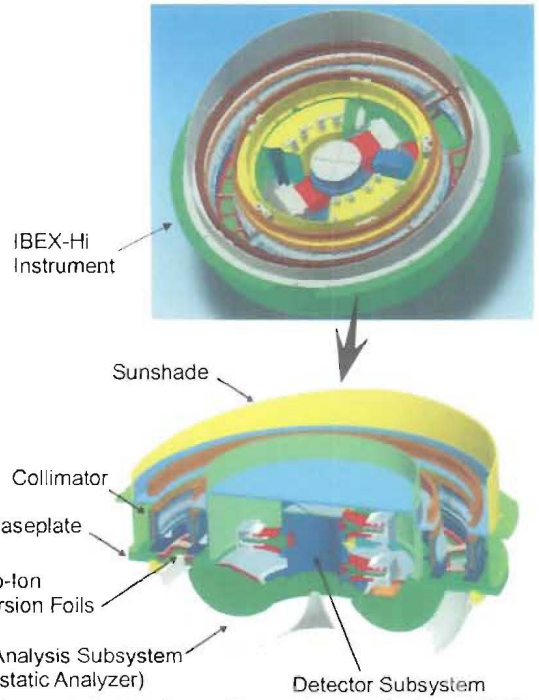

Figure 1. Isometric and section views of the IBEX-Hi instrument.

[1] R&D Engineer, Space Science and Applications Group, P.O. Box 1663, MS-B244.
[2] R&D Engineer, Satellite Mechanisms Group, Dept 2617.

plates directs the ions to the detector section. The electric field imposed between the two ESA plates is selected so that only ions within a specific mass-energy band can enter into a centralized detector section. The detector employs carbon foils which emit electrons when the ionized ENAs pass through them. Positively-charged channel electron multipliers (CEMs) positioned on the side of the detector, collect the electrons and amplify the signal sufficiently so that it can be identified and recorded by the detector's electronics.

The mechanical design of the IBEX-Hi instrument proved to be extremely challenging, primarily due to its large size relative to previously launched electrostatic analyzer instruments[1-3]. The imposed functional and environmental requirements combined with limited spacecraft accommodations, dictated complex mechanical geometries, unique material and surface finish selections, and difficult fabrication processes. Furthermore, the intended space mission required detailed structural and thermal analyses combined with extensive environmental testing to qualify the mechanical design. In a previous study[4], detailed thermal analyses and testing of a prototype IBEX-Hi instrument were reported and thus will not be discussed here.

This paper presents the details of the mechanical design and several of the more difficult production processes, including the manufacturing of the ESA plates and the assembly of the ultrathin carbon foils. Various mechanical prototyping approaches of the ESA plates and carbon foils are reviewed along with the problems and successes encountered with each. Next, the dynamic acoustic and random vibration testing of a full-scale prototype instrument are discussed. Finally, the design and production modifications for the flight instrument components, based on the results of analyses and environmental tests, are presented.

II. Mechanical Design and Prototype Fabrication

Figure 2 is an exploded view of a preliminary design of the IBEX-Hi instrument, minus the collimator and the detector electronics. The backbone of the instrument is the baseplate, a prototype of which is displayed in Fig. 3. The baseplate houses the ENA conversion foils, serves as the mounting structure for the other instrument components, and provides the mechanical interface to the spacecraft. Al-6061-T6 was selected as the baseplate material for its light weight, high strength, large thermal conductivity, and desirable machining properties. Finite element modal analyses were performed in conjunction with the CAD modeling of the baseplate to minimize its weight and provide sufficient stiffness to maintain a first mode resonance frequency greater than 300 Hz. High precision machining was required to ensure accurate positioning of the electro-optical components and minimize interference problems with the multiple fastener interfaces.

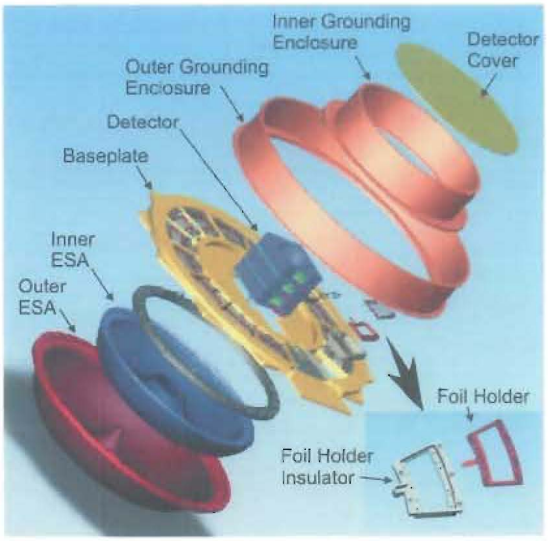

Figure 2. Exploded CAD view of the IBEX-Hi prototype instrument.

Attached to the underside of the baseplate are the two concentric ESA plates, shown in Fig. 4. Instrument performance requirements and mass limitations dictated a relatively large aspect ratio for the ESA plates (20 to 35 cm in diameter and 0.4 to 0.9 mm in thickness). This aspect ratio, combined with the unique shape of the ESA plates, created a considerable challenge in their manufacturing. Several fabrication techniques were explored, including spin forming, stamping, machining, and electroplating. The spin forming and stamping techniques utilized opposing steel mandrels with meshing interface geometries that mirrored those of the corresponding ESA plates. 0.32 cm (0.125 in.) thick Al-6061 plates were pressed over a spinning or stationary mandrel with a second mandrel to form the plate into the desired ESA geometry. For the inner ESA, both the spin forming and stamping techniques generated the geometry from a single piece of plate stock. For the more complicated outer ESA, the spin forming method was also

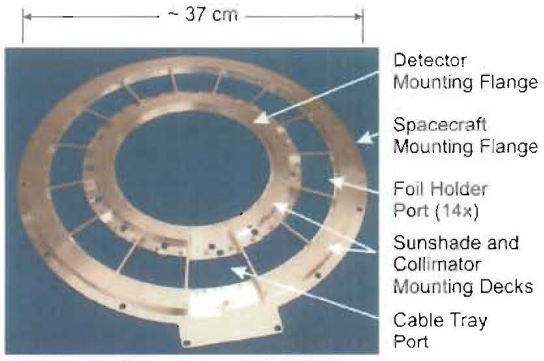

Figure 3. Prototype baseplate.

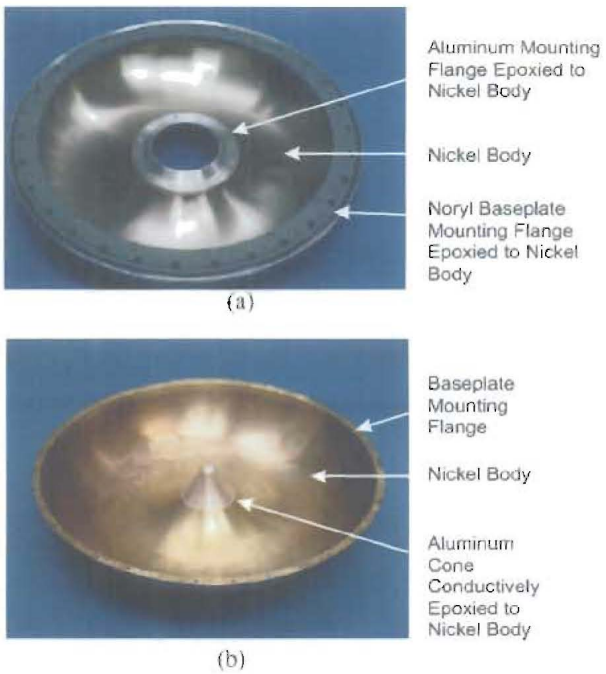

Figure 4. Prototype (a) inner ESA and (b) outer ESA.

successful in generating the geometry from a single plate. However, the stamping method required the center and periphery portions of the outer ESA to be shaped individually and then welded together to make the final geometry. Both fabrication techniques produced the two ESA geometries, but did so with considerable geometrical variations, residual stresses, and porous welds (for the stamped outer ESA). It became evident that either fabrication technique would need to be refined and would require post-forming machining, stress relieving, and enhanced welding techniques to obtain the desired geometrical tolerances. In parallel with these approaches, an electroplating process was used to form 0.4 mm thick inner and outer Nickel ESA plates on aluminum forms. Following the electroplating, the aluminum forms were rapidly cooled with liquid nitrogen in an attempt to release the ESA plates from the forms. For the inner ESA, this process worked without incident. However, for the outer ESA, the center-most material did not separate from the form and had to be cut to release the majority of the outer ESA from the form. An aluminum cone was machined and secured to the remainder of the outer ESA with conductive epoxy. The two electroplated ESAs are shown in Fig. 4.

Distributed around the periphery of the baseplate are fourteen ENA conversion foil assemblies and a Noryl cable conduit for the detector's electrical cabling. As mentioned previously, each foil assembly possesses an ultra-thin carbon foil that is responsible for electron charge exchange as an ENA passes through it. Figure 5 presents a CAD model of a typical foil holder assembly in both exploded and assembled states. The foil holder consists of an electro fromed Nickel screen (12.7 μm diameter wire with a pitch of 131 wires/cm) stretched between two aluminum (Al-6061-T6) frames. A 0.25 cm high step on the lower frame allows the screen to be bent and stretched tight as the two frames are brought together with a complement of screws. Once the screen is stretched tight, a thin carbon foil (50-100Å thick) is deposited onto the screen using the process described in Ref. 5. The aluminum frame assembly is secured with screws to an electrically insulating Noryl (GN-30) cradle which in turn is mounted to the baseplate. The Noryl insulator is required because the baseplate is electrically grounded and the foil holders are energized to several hundred volts to provide an acceleration force for the ions as they exit the foil.

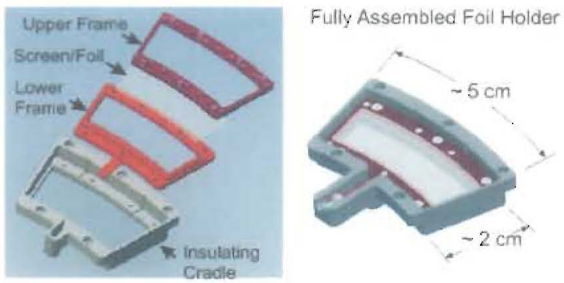

Figure 5. Exploded and assembled CAD model views of the foil holder assembly.

Previous acoustic tests performed by one of the authors[6] with a prototype IBEX-Hi instrument, resulted in catastrophic failure of several foils on the 0.25 cm high step frame, as displayed in Fig. 6. These foil failures lead to a design evolution involving multiple foil holder geometries described below and incorporated in the environmental tests described in this manuscript. It was speculated that the tight fit of the upper and lower frames, combined with the 0.25 cm high step, led to plastic deformation or ultimate failure of the screen material outside of the direct view of the foil holder assembler. Several foil holder

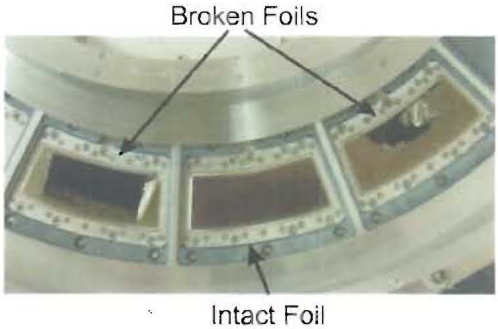

Figure 6. Failure of two 0.25 cm step foil holder frames in a previous acoustic test[6].

assemblies were taken apart and the screens were laid flat and inspected. All of the screens exhibited signs of plastic deformation, as evident in the rippled stress contours remaining in the deformed screen, as shown in the upper right photo of Fig. 7(b). Furthermore, 20% of the screens had small tears in the vicinity of the step interface. To overcome this mechanical deficiency, foil holders were produced with a shorter 0.08 cm right angled step, a 0.08 cm tall and 20° tapered step, and no vertical step. Reducing the step height from 0.25 to 0.08 cm reduced the stresses in the screen considerably, as shown in Fig. 7(b). Complete elimination of the step obviously removed all stresses in the screen (see photo in lower right of Fig. 7(b)) and lead to the concept of the welded frame in which a Ni screen was stretched and held between a stainless steel 304 lower frame and upper shim that were spot welded together (see photo in lower left of Fig. 7(a)). The welded frame design eliminated the need for accurate machining tolerances between the mating frames as well as the need for seventeen assembly screws, but required a small increase in overall weight. One final modification to the foil holder involved the addition of a center stiffening rib, which added central support to the screen. Examples of the center rib on the stepped frame and the flat welded frame are displayed in Fig. 7(a). Each of these frame designs was included in the first round of acoustic and vibration testing, discussed in the next section, to assess the mechanical integrity of the different design features.

Figure 7. (a) Foil holder design evolution including stepped frame, ribbed-stepped frame, and welded ribbed frame design and (b) stress contours in flattened screens that have been previously stretched in various foil holder assemblies.

Attached to the upper surface of the baseplate above the conversion foils, is a toroidal-shaped collimator. The collimator is comprised of a stack of twelve aluminum aperture plates, each photo-etched with a continuous pattern of hexagonal openings to provide a visual transmission of 70%. Each of the aluminum plates is separated from its neighbor and from the instrument baseplate by ceramic insulating spacers. A mechanical representation of the collimator geometry, used in the IBEX prototype thermal testing of Ref. 4, is shown in Fig. 8. While this collimator prototype was acceptable for thermal testing, it was too heavy and non-representative for acoustic and vibration testing. Cost limitations prevented a suitable prototype from being constructed in time for the environmental testing discussed in this document. Positioned on either side of the collimator are two concentric aluminum sunshades, which shield the collimator and conversion foils from direct sunlight and cosmic rays to suppress background noise.

In the center of the baseplate is the mounting interface for the detector assembly.

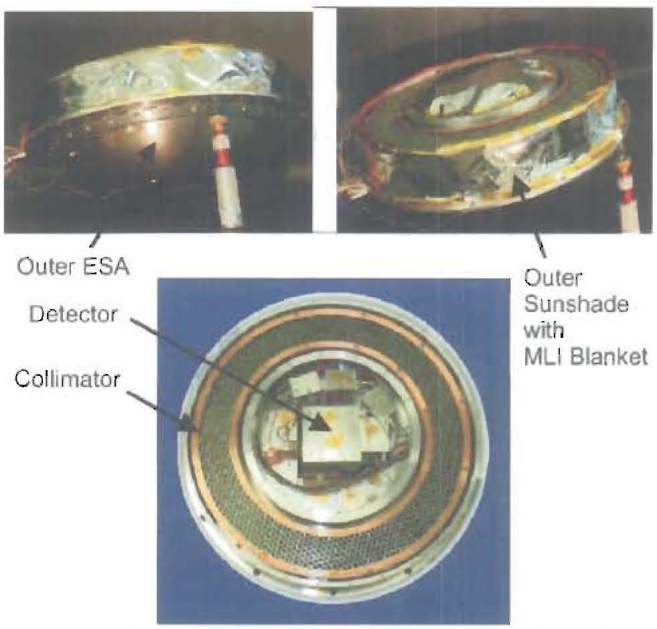

Figure 8. Prototype IBEX-Hi instrument utilized for previous thermal[4] and functional tests, showing the collimator and functional detector subsystems.

The detector subsystem, shown previously in Fig. 1, consists of two pie-shaped electronics modules located on either side of a cylindrical detector column. The detector column houses two carbon foils and three channel electron multipliers mounted to a stacked assembly of three aluminum cylinders. A functional prototype detector, shown in Fig. 8, was assembled for preliminary functional tests of IBEX-Hi. However, this prototype detector was not suitable to withstand the large mechanical loads of the acoustic and random vibration testing environments and hence was replaced with a suitable mass model for the dynamic testing.

Figure 9 displays a prototype IBEX-Hi instrument which was used for the acoustic and random vibration tests discussed in this study. As mentioned above, the collimator was omitted and the detector was replaced with a representative mass model.

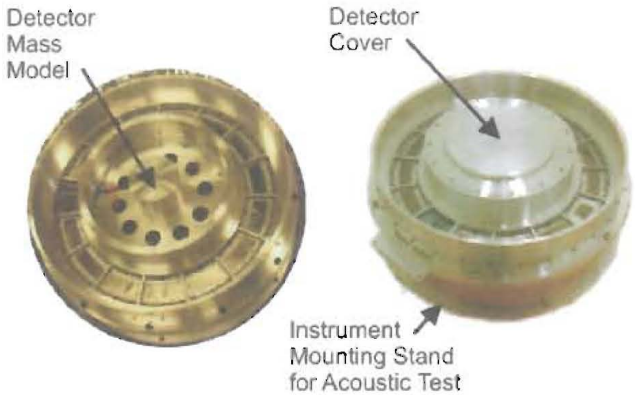

Figure 9. Prototype IBEX-Hi instrument utilized for current acoustic and random vibration tests.

III. Environmental Testing Methods

The following section outlines the dynamic environmental tests conducted on the IBEX-Hi prototype instrument shown in Fig. 9. These preliminary qualification tests were performed to assess the integrity of the mechanical design and provide empirical data to validate numerical and analytical structural models. Two different types of dynamic environmental tests were performed on the instrument assembly, including acoustic and random vibration. The Acoustic Sound Pressure Level (SPL) and Power Spectral Density (PSD) spectrums that the instrument was subjected to for the acoustic and random vibration test, respectively, are displayed in Fig. 10. Note in Fig. 10 that two different SPL profiles were employed in several phases of acoustic testing of the IBEX-Hi prototype instrument. The two different SPL profiles were produced during concurrent dynamic studies by the IBEX Spacecraft provider in which the Spacecraft launch conditions and dynamic environment had evolved. The higher and more conservative SPL profile was used in previous IBEX-Hi acoustic testing[6] and was also used in Phase 1 of the acoustic testing of the present study discussed below. The lower and more refined SPL profile was used in Phases 2 and 3 as outlined in the next section. Specific test durations, instrument orientations, and additional configuration details are discussed below.

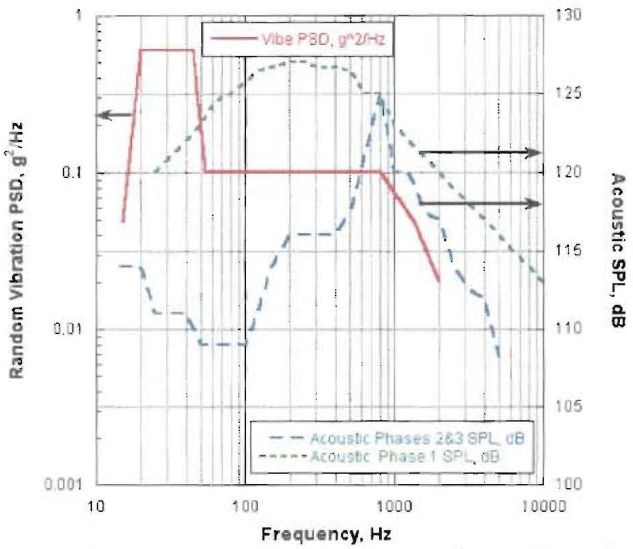

Figure 10. Random vibration Power Spectral Density (g^2/Hz) and Acoustic testing Sound Pressure Level (dB) profiles used in dynamic testing. Integrated PSD as well as Phase 1 and Phase 2/3 overall SPL values for these profiles are 12.3 g_{rms}, 138 dB, and 131 dB, respectively.

A. Random Vibration Testing Methods

Figure 11 displays the experimental set-up and instrument configuration for the random vibration tests. The prototype instrument was mounted on a vibration test fixture which consisted of a hollow aluminum cylinder (wall thickness = 5.08 cm, height = 15.24 cm) bolted to a 5.08 cm thick aluminum plate. The test fixture assembly was numerically modeled to ensure that its fundamental frequency was greater than 2 kHz, the maximum frequency of the random vibration PSD. This ensured a seamless transition between the shaker mechanism and the instrument's baseplate mounting interface. An Unholtz-Dickie T4000 electrodynamic single axis shaker and slip table were used to provide the random vibration excitation. Four single axis Endevco 2221D piezoelectric accelerometers were mounted to the aluminum fixture plate with a high strength adhesive to serve as the control accelerometers in the Y and X directions (2 per axis). Two single axis Endevco 2221D

accelerometers and two triaxial accelerometers (each built up with three 2250A/AM1-10 accelerometers) were mounted to the prototype instrument for response measurements. The accelerometer mounting locations are shown in Fig. 11. Prior to performing the two acoustic tests, the instrument was shaken individually in the Y and X axes (refer to Fig. 11 for coordinates), for a duration of 2.5 minutes per axis. The symmetry of the instrument allowed the Z axis testing to be eliminated from the test program. Prior to and immediately following each of the X and Y axis vibration test, a low-level random vibration survey (0.004 g^2/Hz from 15 to 2000 Hz) was performed to search for resonance changes (frequency or amplitude) which would be indicative of a mechanical failure.

B. Acoustic Testing Methods

Figure 12 displays the experimental setup for the acoustic testing. The prototype instrument was mounted to an aluminum spool piece and positioned several feet off of the floor on an acoustically transparent bench. Eight electromagnetic acoustic speakers, including two JBL M-4 mid-bass, two Maryland Sound SB1000 sub-bass, and four Maryland Sound VA4 full-range speakers, and three control microphones (Brüel & Kjaer, Model 4134) were placed around the horizontal periphery of the instrument on 1m and 0.25m radii, respectively. Two additional response microphones (Brüel & Kjaer, Model 4138) were integrated with the instrument, as shown in Fig. 12, to observe any amplification or damping of the acoustic load as a result of the instrument geometry and design. One of these microphones was placed 1.75 cm above the baseplate, while the second microphone was inserted 1.75 cm below the baseplate by replacing one of the foil holders with the microphone body and its corresponding foam holder, cut to fit the gap between the microphone body and baseplate. The entire test set-up was positioned within a reverberant acoustic chamber to provide isotropic acoustic loading. Three successive tests, referred to as Phase 1, 2, and 3, were performed on the IBEX-Hi prototype, each using a different complement of foil holders. In phase 1, the higher SPL profile of Fig. 10 was utilized, while for phases 2 and 3, the lower SPL profile was implemented. In each test, the total acoustic exposure period was 150 seconds. Phase 1 was performed in five increments of 30 seconds each, while phases 2 and 3 were both performed in two increments of 75 seconds each. A 5 minute dwell period was required between the various increments to

(a)

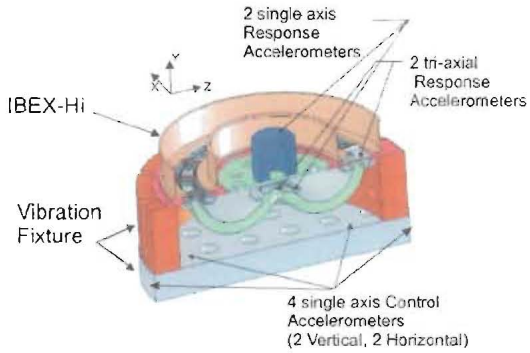

(b)

Figure 11. (a) IBEX-Hi prototype mounted in vibration test fixture and secured to shaker slip table and (b) CAD section view of instrument and vibration fixture showing control and response accelerometer mounting locations.

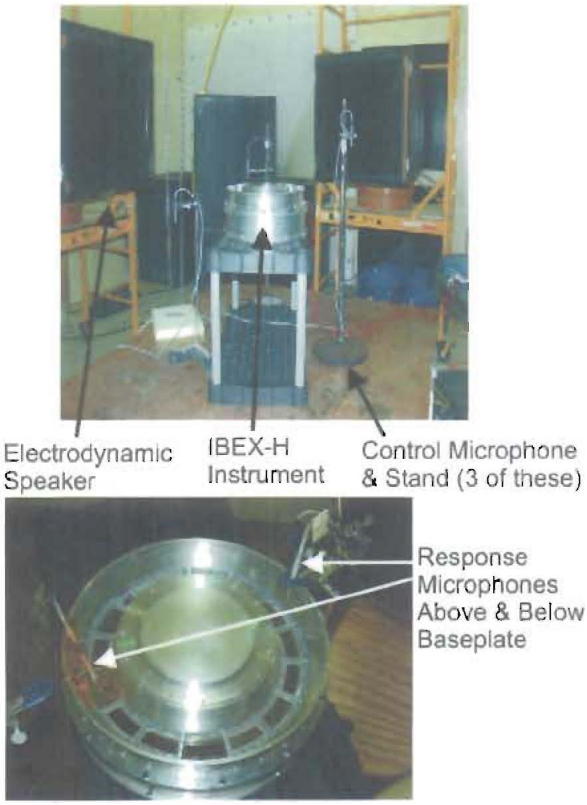

Figure 12. Photographs of the test configuration for the acoustic testing of the IBEX-Hi prototype.

allow the electrical power amplifiers driving the speakers, to cool. Since mechanical failures from acoustic or vibration testing can usually be attributed to fatigue[7], this interval testing strategy was determined to be adequate for the types of qualification tests being conducted. Phases 1 and 2 each utilized a variety of foil holder configurations including four of the 0.25 cm step frames, three of the 0.08 cm step frames, one 20° tapered frame, two flat screwed frames, and three welded frat frames. Phase 3 employed a complete complement of only the welded flat frame design.

IV. Test Results and Assessments

A. Random Vibration Test Results

The X and Y axis random vibration tests were completed without any visible signs of mechanical failure of the prototype instrument. Furthermore, the pre and post low level vibration surveys did not show any resonance shifts nor change in response amplitudes, suggesting that the structure maintained its initial configuration. Figure 13 is a representative response PSD profile obtained during the Y axis vibration test. The control input PSD bounds (+/- 3 dB) are shown as the outer-most dashed profiles in the figure. As the profile indicates, the detector baseplate has large responses at several frequencies, as would be expected for such a structure with large aspect ratio components and many bolted interfaces. Table 1 attempts to summarize many of the response PSD profiles that were obtained in the two vibration tests. Note that the *transfer function* listed in Table 1 is defined as the square root of the ratio of the response PSD to the input PSD at the frequency of interest and serves as a measure of force amplification due to resonances in the structure. Also note that the Z response accelerometers did not reveal any significant motions that the X response accelerometers had already captured, and thus their data is not displayed in Table 1. For the X direction vibration test, the instrument did exhibit several large amplifications in both the X and Y directions in the frequency range of 190 to 480 Hz. Both ESA plates appear to rock back and forth and thus couple the input energy into a multi-directional output, which is then transmitted to the baseplate and the rest of the instrument. This is even more evident in the transfer functions for the Y direction vibration test. The data indicates significant drumming of the baseplate, inner ESA, and outer ESA in the frequency range of 190 to 480 Hz. The large transfer functions of 47.0 of the baseplate at 280 Hz and 32.4 of the outer ESA at 230 Hz, suggest that additional stiffening of the structure may be required. Higher order modes (> 800 Hz) of these large accelerations are evident at all of the accelerometer locations and cross coupling between axes is obvious in the outer ESA accelerometer response data (e.g. Outer ESA X responds to Y input). Never-the-less, the prototype structural design appears to be fairly sound for the intended dynamic environment with only modest design changes to provide additional stiffening and strength.

Future finite element structural modeling, validated with the empirical response spectrums from this study, would be required to predict detailed stress levels and assist in design modifications to optimize the structural integrity of the instrument.

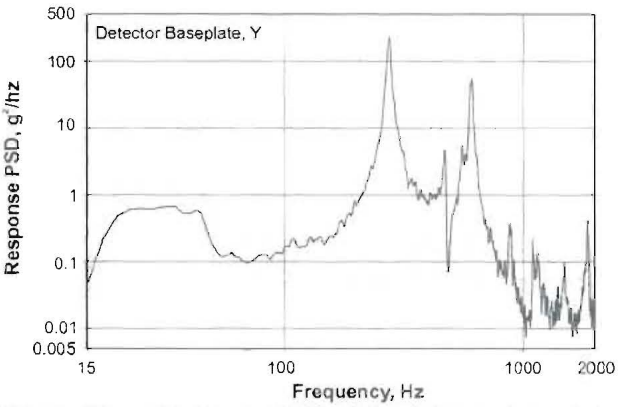

Figure 13. Response PSD of the detector baseplate in the Y direction for the Y PSD input profile.

Table 1. Summary of the major response frequencies and transfer functions for various measurement locations for the X axis and Y axis random vibration tests.

	X Direction Vibe		Y Direction Vibe	
Measurement Location & Direction	Frequency (Hz)	Transfer Function	Frequency (Hz)	Transfer Function
Detector Baseplate, Y			280	47.0
	480	10.1	480	7.1
			620	24.5
			1800	4.5
Outer ESA, X	280	19.5	280	3.9
			320	3.2
			1200	25.0
			1600	6.1
Outer ESA, Y			230	32.4
	280	20.2	280	12.2
			620	4.7
			800	3.2
Inner ESA, Y	190	37.4	190	11.8
			250	8.9
			650	3.2
Cable Tray, Y			250	11.4
	650	16.7	650	17.2
	1100	7.8	1100	5.8
			1650	12.9

B. Acoustic Test Results

The phase 1 acoustic tests resulted in several foil failures during different 30 second test intervals. The failures took place on all of the foil holder design configurations with the exception of the welded flat frame design. Figure 14 shows photographs of broken foils on both a 0.08 cm rectangular step and a 0.08 cm tapered step foil holder assembly. Note that when a foil failed, it was replaced with an intact foil during the 5 minute dwell period between test intervals. The replacement of the broken foils was necessary to prevent bypass acoustical venting through the broken foil. All of the foils that survived the test showed signs of stretching and rippling across their once smooth surface, suggesting that some plastic deformation of the screen elements did occur.

Response microphone data indicated that the instrument amplified the overall sound pressure level in the region immediately above and below the foils by approximately 2.5 dB and 5.1 dB, respectively.

Phase 2 was nearly a repeat of the phase 1 test, except that the test level was reduced. In this case, all of the foils remained intact. As with the foils that survived the phase I tests, the phase 2 foils exhibited some permanent rippling in their surfaces.

It was concluded from the phase 1 and phase 2 testing that the welded flat frame design exhibited the best characteristics to survive the acoustic environment, minimized the use of fasteners, and offered the greatest repeatability and consistency in fabrication and assembly. To demonstrate that a complete set of welded flat frame foil assemblies could be produced and pass the acoustic test, a complete complement of welded frames was used in the phase 3 acoustic test. All 13 foils survived the phase 3 test, although two of the assemblies exhibited single small tears on the order of 2 mm near the edges of each foil and the remainder displayed slight rippling of the foil surface. Figure 15 shows photos of one such foil holder assembly from before and following the phase 3 acoustic test.

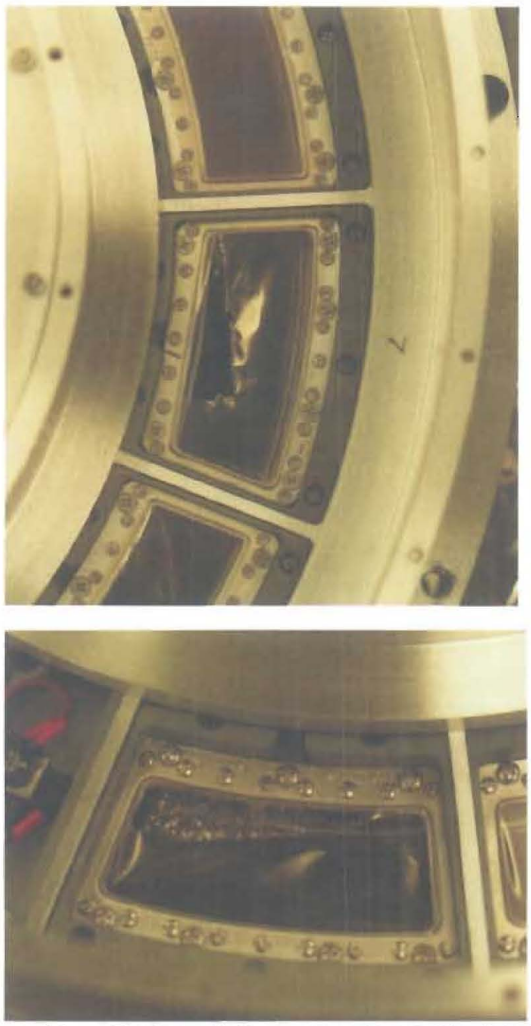

Figure 14. Broken foils encountered during the phase 1 acoustic tests.

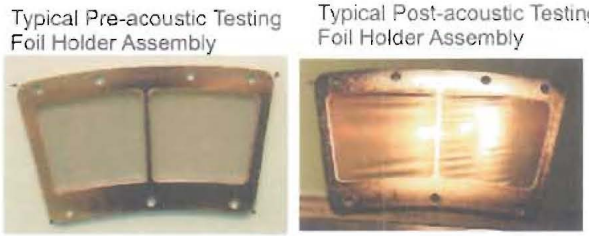

Figure 15. Photographs of a welded frame foil holder before and after the phase 3 acoustic test.

V. Conclusions

This manuscript described many of the challenges associated with the mechanical design, fabrication and dynamic environmental testing of a prototype spacecraft instrument. The integration and iterative nature of the design, fabrication, prototyping, and testing activities was demonstrated and the successes as well as the failures were shared.

Studies are ongoing to understand and characterize the failure mechanisms of the carbon foils. Empirical frequency measurements of the foils along with fatigue analysis models are being combined with the acoustic response data of this study in an attempt to achieve this goal. At the same time, the final design and development of the IBEX-Hi flight instrument is progressing, taking full advantage of the lessons learned from the prototype instrument design and testing activities described in this manuscript.

Acknowledgments

The authors would like to express their genuine thanks and appreciation to Herbert Funsten for his guidance and support through the course of this project. Many engineers, designers, technicians, and support personnel at Los Alamos National Laboratory, Southwest Research Institute, and Sandia National Laboratory contributed to the success of this study. Finally, the financial support of NASA made this project possible and for that we are truly grateful.

References

[1]Norholt, J. E., Young, D. T., and Funsten, H. O., "Plasma Experiment for Planetary Exploration (PEPE) on DS1," *IEEE Aerospace Conference*, IEEE, Big Sky, Montana, 2000.

[2]Bame, S. J., et al., "The ISPM Solar-Wind Plasma Experiment," European Space Agency Special Publication SP-1050, pp. 47-73, 1983.

[3]Hahn, S., et al., "A Validation Payload for Space and Atmospheric Nuclear Event Detection," *IEEE Transactions on Nuclear Science*, Vol. 50, No. 4, 2003, pp. 1175-1181.

[4]Jones, D. C., and Bernardin, J. D., "Thermal Modeling and Experimental Verification of the Interstellar Boundary Explorer's High Energy Neutral Atom Imaging Instrument (IBEX-Hi)," *Proceedings to the AIAA Infotech@Aerospace 2007 Conference and Exhibit*, AIAA-2007-2949, Rohnert Park, CA, 2000.

[5]McComas et al., "Ultrathin (~10 nm) Carbon Foils in Space Instrumentation," Review of Scientific Instruments, Vol. 75, No. 11, 2004, pp. 4863-4870.

[6]Baker, D. R., and Ramsey, M. J., "Intersteller Boundary Explorer-High Energy (IBEX-Hi) Flight Instrument Prototype Acoustic Test Report," ATAC-23-15-82002101, ManTech Int. Corp., NASA GSFC, Greenbelt, Maryland, May, 2004.

[7]Steinberg, D., *Vibration Analysis for Electronic Equipment*, 3rd ed., John Wiley & Sons, New York, 2000.